International Journal for Housing Science and Its Applications
Publish August 10, 2025. Volume 46, Issue 4 Pages 86-102

https://doi.org/10.70517/ijhsa46407

Power system balance calculation and optimization method considering distributed power sources and electric vehicle charging loads

Wei Ye[1,*], Xiaoyan Zhang[1], Jialu Wei[1], Xuling Jiang[1] and Xingxing Zhou[2]
[1] Hangzhou Electric Power Design Institute Co., LTD., Hangzhou, Zhejiang, 310012, China
[2] Chongqing Xingneng Electric Co., LTD., Chongqing, 400039, China
Corresponding authors: (e-mail: 15696198698@163.com).

Abstract In this paper, distributed power supply and electric vehicle charging load are studied in depth, and the distributed power supply output model and electric vehicle charging load prediction model are constructed, which are integrated into the power system balance calculation model. In the framework of traditional power balance calculation, flexible calculation method is introduced for improvement, a new power system model is constructed, and a new power system power balance method based on flexible calculation is proposed. The application of the flexible calculation method in power systems is understood through the flexible balance calculation and example study of typical regional power grids.The variation interval of the load flexibility parameter in region A is [20350, 25000] MW, and the minimum value on the left side of the flexibility inequality (24524.6) is larger than the maximum value on the right side (23875.6), which realizes the flexible balance.The annual load of the power system of province Z is dominated by the summer and winter as the The annual load of the power system in Province Z is peaked in summer and winter, and troughs in spring and fall. The daily load basically shows the pattern of “double peaks and double valleys”. The UHV DC corridor in Province Z delivers power according to the 100/75 curve, with 100% capacity in January, July, August and December, and 65% capacity in other months. The UHV AC channel delivers power on a 100/70/55 curve throughout the year. Photovoltaic output is large in spring and small in winter, and the maximum output in a day is around 13:00. Wind power output is large in winter and small in summer, with large output at night and small output during the day.

Index Terms distributed power, charging load, power system, balance calculation, flexible calculation

I. Introduction

In the face of energy and environmental pressures, the development of electric vehicles (EVs) and the promotion of low-carbon transportation are hotspots of concern for the governments of China and major developed countries around the world, and all countries have increased their policy support for EVs [1]-[3]. In the traditional electric power system, the power supply mainly relies on traditional energy sources such as coal and oil, while the charging demand of electric vehicles increases the pressure on the grid load [4]-[6]. The disorderly charging behavior of large-scale EVs in time and space will not only cause the phenomenon of “peak on peak” and increase the peak-valley difference of the power grid, but also may cause local overloading of the power grid, line congestion, and other problems, which will bring about an impact on the stable operation of the power grid [7]-[10]. Reasonable power system balance calculation and optimization strategy is the key to ensure the safe and stable operation of power system [11], [12].

Power system balance refers to the equilibrium state between supply and consumption in the power system, and the reliability of power supply and potential problems can be assessed by analyzing the balance of the power system [13], [14]. And power system balance calculation is one of the important contents of power system planning and operation, which is mainly used to determine the supply and demand balance of the power system and make corresponding adjustments and optimization according to the balance [15]-[17]. The results of power power balance calculation directly affect the stability, reliability and economy of the power system [18], [19]. Electric vehicle charging load power system optimization is to ensure the stability of power supply, the power system must be able to adjust the power generation in time to meet the load demand of electric vehicles, only to maintain a balanced relationship between power generation and load to ensure the reliability of power supply, to avoid the problem of insufficient or excess power [20]-[23].

For the consideration of distributed power supply and EV charging load, this paper first constructs a distributed power supply model that includes wind power and photovoltaic power generation, and an EV charging load prediction model that covers buses, cabs and private cars. Then, a new power system model framework is designed on the basis of the traditional power support electric power balance calculation. According to the system electric power quantity and balance conditions, a flexible calculation strategy is added for optimization processing, and a new electric power system power balance method based on flexible calculation is proposed. The balance calculation method proposed in this paper is used to flexibly calculate the charging load of the power grid in a typical area, and compared with the traditional method. Finally, the grid load characteristics and new energy output characteristics are discussed through an example study.

II. Distributed power and electric vehicle charging load forecasting models

II. A. Distributed Power Output Model

Distributed power sources have become the main direction of future grid development and have been integrated into the grid on a large scale due to their flexible power generation methods and high operational efficiency [24]. Compared with traditional fossil fuel power stations, distributed power sources such as wind power and photovoltaic power have the advantages of small capacity, green and renewable. However, as the output of these distributed power sources is affected by natural factors such as weather and environment, it shows strong randomness, seasonality and volatility, which will bring uncertainty and instability to the operation of the traditional power grid. At the same time, the load nodes in the distribution network are also affected by human factors and have timing characteristics. In this paper, distributed power characteristics and electric vehicle charging loads are fully considered, and distributed power is combined with traditional power generation methods and incorporated into the balance calculation of the power system.

II. A. 1) Wind power output modeling

Wind power is a clean, renewable energy source with a potentially huge market and development prospects. Wind turbines generate mechanical energy by converting wind energy, which is then converted into electrical energy by a motor, and this process requires wind speed control to ensure that the output of the wind turbine can match the requirements of the power grid. In order to better understand the effect of wind speed on the output of wind turbine, the corresponding output model needs to be established. Commonly used probabilistic output models for wind turbines include the Weibull distribution, the Gumbel distribution model, the Rayleigh distribution model, and so on.

The output uncertainty of wind turbine mainly originates from the intermittency and randomness of the wind speed itself, the most used wind speed model is the Weibull distribution model [25], the probability density function (PDF) of the wind speed v is $f(v)$, and the cumulative distribution function is $F(v)$, with the following expression:

$$f(v)=\frac{k}{c}\left(\frac{v}{c}\right)^{k-1}\exp\left[-\left(\frac{v}{c}\right)^{k}\right] \tag{1}$$

$$F(v)=1-\exp\left[-\left(\frac{v}{c}\right)^{k}\right] \tag{2}$$

where k is the shape parameter of the Weibull distribution, describing the shape of the probability density function of wind speed. c is the scale parameter of the Weibull distribution, described as the average wind speed in a certain period of time.

The output power of the wind turbine is related to the wind speed and the rotational speed of the wind turbine, and the wind speed is affected by the weather and geography showing strong uncertainty. The relationship between wind turbine generating power and wind speed is given in the following equation:

$$P_{WT}^{r}=0.5N_{WT}\rho A_{WT}v_{r}^{3}\eta_{WT} \tag{3}$$

$$P_{WT}(v)=\begin{cases}0 & v\le v_{ci},v\ge v_{co}\\ P_{WT}^{r}\dfrac{(v-v_{ci})}{(v_{r}-v_{ci})} & v_{ci}\le v\le v_{r}\\ P_{WT}^{r} & v_{r}\le v\le v_{co}\end{cases} \tag{4}$$

where $P_{\mathrm{WT}}^{\mathrm{r}}$ is the rated output power of the wind turbine (kW), $P_{\mathrm{WT}}(v)$ is the actual output power of the wind turbine (kW), N_{WT} is the unit's quantity, ρ is the air density $\left(\mathrm{kg/m^3}\right)$, A_{WT} is the area of the wind turbine blades $\left(\mathrm{m^2}\right)$, and η_{WT} is the coefficient of utilization of wind energy, also known as the efficiency of energy conversion, which indicates the ratio of the energy gained by the wind turbine from the wind to the theoretical maximum energy that can be gained from the wind energy. The ratio of the energy obtained from the wind by the wind turbine to the maximum energy that can be obtained from the wind theoretically. Generally speaking, the value of η_{WT} is between 0.35-0.50, v_{r} is the rated wind speed $(\mathrm{m/s})$, v_{ci} is the cut-in wind speed $\mathrm{m/s}$, and v_{co} is the cut-out wind speed $(\mathrm{m/s})$.

The output power of the wind turbine P_{WT} is affected by a variety of factors such as the rated wind speed v_{r}, the cut-in wind speed v_{ci} and the cut-out wind speed v_{co}, etc. When the actual wind speed is smaller than the cut-in wind speed or larger than the cut-out wind speed $(v \le v_{ci}, v \ge v_{co})$, the turbine output power is zero. When the actual wind speed is greater than the cut-in wind speed but less than the rated wind speed $(v_{ci} \le v \le v_r)$, the output power of the fan is proportional to the wind speed. When the actual wind speed is greater than the rated wind speed and less than the cut-out wind speed $(v_r \le v \le v_{co})$, the output power of the fan stays constant and is the rated output power.

II. A. 2) Photovoltaic Power Generation Output Modeling

Distributed photovoltaic power supply refers to the use of solar energy through photovoltaic power generation technology to directly convert solar energy into electrical energy power supply equipment [26], photovoltaic system is composed of photovoltaic modules, inverters, batteries storage and other devices, photovoltaic module is the core part of the photovoltaic power supply, which can be directly converted from solar energy to electrical energy, and power generation power depends directly on the light irradiance. Distributed photovoltaic power supply has the advantages of environmental protection, renewable, flexibility, etc. Secondly, the decentralization of photovoltaic power supply can reduce the transmission loss, improve the efficiency of energy utilization, reduce the degree of dependence on the traditional grid, and have a certain role in promoting the safe and stable operation of the power grid. However, distributed PV power also has some disadvantages and challenges. Since the output of PV power supply is affected by natural conditions such as weather and temperature, the output stability of PV power supply needs to be considered during the planning, siting and installation of PV power supply. Therefore it is necessary to study the modeling and planning of distributed PV systems.

The output power of solar PV units is determined by several factors, mainly including solar radiation intensity, solar panel characteristics and temperature and humidity, etc. The solar radiation intensity is affected by geographic location, seasons and weather conditions, showing strong volatility and uncertainty. Among them, light intensity is the main influence factor affecting PV output. The most commonly used probability model to describe light intensity is Beta distribution, and the probability density function of light intensity I $f(I)$:

$$f(I)=\frac{\Gamma(\alpha+\beta)}{\Gamma(\alpha)\Gamma(\beta)}\left(\frac{I}{I_{\max}}\right)^{\alpha-1}\left(1-\frac{I}{I_{\max}}\right)^{\beta-1} \tag{5}$$

where I is the actual light intensity in $\mathrm{W/m^2}$, $I_{\max}$ is the maximum light intensity, $\Gamma(\cdot)$ is the gamma function, α is the shape parameter of the Beta-distributed probability density function, and β is the Beta-distributed probability density function scale Parameters. It can be calculated based on the expectation μ_I and variance σ_I^2 of the light intensity historical data:

$$\alpha=\mu_I\left[\frac{\mu_I(1-\mu_I)}{\sigma_I^2}-1\right] \tag{6}$$

$$\beta=(1-\mu_I)\left[\frac{\mu_I(1-\mu_I)}{\sigma_I^2}-1\right] \tag{7}$$

If there are N_{PV} solar photovoltaic (PV) panels, the area of a single PV panel is $S_i(\mathrm{m^2})$, and its photovoltaic conversion efficiency is η_{PV}, the output power of the PV unit P_{PV} is denoted as:

$$P_{PV} = I \cdot \sum_{i=1}^{N_{PV}} S_i \cdot \frac{\sum_{i=1}^{N_{PV}} S_i \eta_{PV}}{S_{PV}} \tag{8}$$

$$S_{PV} = \sum_{i=1}^{n} S_i \tag{9}$$

The PDF of the output power of the PV unit is still Beta distribution, which is obtained from Eq. (5) and Eq. (8):

$$f(P_{PV}) = \frac{\Gamma(\alpha+\beta)}{\Gamma(\alpha)\Gamma(\beta)} \left(\frac{P_{PV}}{P_{PV}^{\max}} \right)^{\alpha-1} \left(1 - \frac{P_{PV}}{P_{PV}^{\max}} \right)^{\beta-1} \tag{10}$$

$$P_{PV}^{\max} = S_{PV} \eta_{PV} I_{\max} \tag{11}$$

where $P_{PV}^{\max}$ is the maximum output power (kW) of the PV unit during a period of time, S_{PV} is the total area (m^2) of the PV panels of the PV unit, and $I_{\max}$ is the maximum value of the intensity of the light I during the period.

In actual operation, the output power P_{PV} of the PV unit exhibits two states: saturated and unsaturated. The relationship is given in the following equation:

$$P_{PV} = \begin{cases} P_{PV}^{r} \dfrac{I}{I_r} & I \le I_r \\ P_{PV}^{r} & I > I_r \end{cases} \tag{12}$$

$$Q_{PV} = P_{PV} \tan(\Phi_{PV}) \tag{13}$$

where P_{PV}^{r} is the rated capacity of the PV unit under standard test conditions (STC, light intensity $I = 1000\,\mathrm{W/m^2}$, AQI AM of 1.5, and temperature of $25^{\circ}\mathrm{C}$) (kW), I_r is the rated light intensity, and Φ_{PV} is the PV output power factor angle.

II. B.Electric Vehicle Charging Load Prediction Model

Different types of electric vehicles have different travel characteristics, and the spatial and temporal distribution prediction models are established for different electric vehicle characteristics as shown in Figure 1.

Electric vehicle charging load to 15 minutes for the interval between the notational calculation, that is, a total of 96 load points recorded in a day, each moment of the load can be expressed as:

$$P_t^j = \sum_{i=1}^{n} p_{r,t}^j, \quad 1 \le t \le 96 \tag{14}$$

where P_t^j denotes the charging power of all EVs at j node at t moment, n is the number of EVs, and $p_{r,t}^j$ denotes the charging power of the i th EV at j node at t moment.

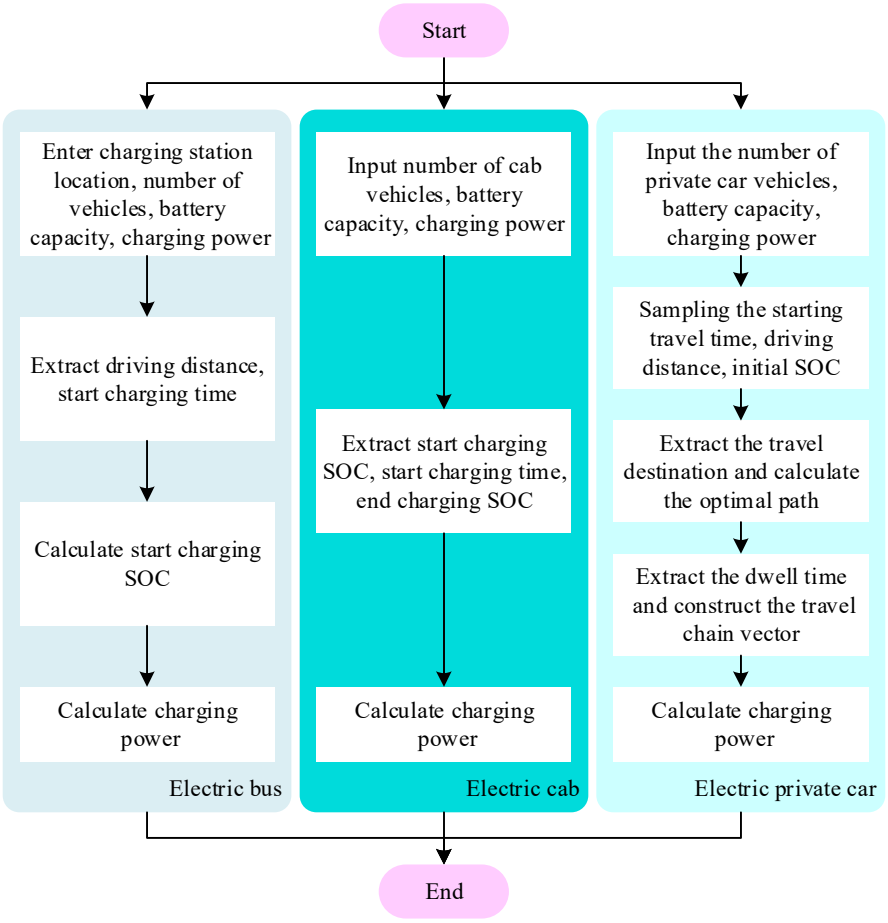

Figure 1: Spatial-temporal distribution prediction of charging loads of different types of EVs

II. B. 1) Prediction Model of Spatial and Temporal Distribution of Charging Load for Electric Buses

Electric buses have fixed bus charging stations with the following steps for spatio-temporal prediction of charging load:

Step 1: Determine the location of electric bus charging station, input the number of electric buses, charging power, battery capacity.

Step 2: Based on Monte Carlo, extract the driving distance of electric buses and the characteristic variables of the moment of starting charging.

Step 3: Calculate the SOC value at the start of charging. The calculation formula is:

$$SOC_e^{bus} = \frac{C - \beta l_{bus}}{C} \tag{15}$$

where C is the battery capacity, β is the power consumption per unit mileage, and l_{bus} is the traveling distance.

Step 4: Calculate the electric bus charging power and calculate the electric bus charging power according to equation (14).

II. B. 2) Electric Taxi Charging Load Spatio-Temporal Distribution Prediction Model

The charging location of electric cabs has randomness and is considered to have equal probability of charging possibility at any node, so each electric cab is considered to randomly select a node for charging. The steps of its charging load spatio-temporal prediction are as follows:

Step 1: Input the number of electric cabs, charging power, and battery capacity.

Step 2: Based on Monte Carlo, extract the start charging SOC, start charging moment, and end charging SOC characteristic variables of electric cabs.

Step 3: Calculate the charging power of electric cabs and calculate the charging power of electric buses according to equation (14).

II. B. 3) Prediction model for spatial and temporal distribution of charging loads of electric private cars

The travel of electric private cars has a certain regularity, which can realize all the simulation of the travel process, and its charging load spatio-temporal distribution prediction steps are as follows:

Step 1: Input the number of electric private cars, charging power, and battery capacity.

Step 2: Based on Monte Carlo, extract the starting travel moment, traveling distance, and starting charging SOC characteristic variables of electric private cars.

Step 3: Randomly extract the travel destinations of private cars according to the above four travel types, select the path to each destination based on Dijkstra's algorithm, and extract the residence time at each destination.

Step 4: Calculate the elapsed time for private cars to go to different destinations and construct the travel chain vector for each private car.

Where the travel chain vector is schematically shown in Figure 2. Where NMN is the trip from point N to point M and back to point N. This travel chain includes the length of stopping time $t_{p,nn}$ at point N, the departure time $t_{d,nm}$ to point M, the driving distance d_{nm}, and the arrival time $t_{a,nm}$, and the length of stopping time $t_{p,mm}$ at point M, and the departure time $t_{d,mn}$ to point N, and the driving distance d_{mn}, arrival time $t_{a,mn}$.

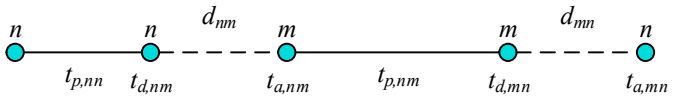

Figure 2: Diagram of 2-level travel chain vector

The elapsed time duration t_l of an electric private car is calculated as:

$$t_l = t_{a,nm} - t_{d,nm} = \frac{d_{nm}}{v} \tag{16}$$

where $t_{a,nm}$ denotes the moment of departure from the current location, $t_{d,nm}$ denotes the moment of arrival at the destination, d_{nm} denotes the distance between the journeys, and v denotes the traveling speed, which is taken as 40kkm/h.

Step 5: Determine whether the charging demand is generated or not, and record the charging information of each electric private car in 15-minute intervals.

Step 6: Calculate the charging power of the electric private car.

III. Power system balance calculation model

III. A. Calculation method for power support electric power balance

III. A. 1) General computational framework

Since distributed power sources have great uncertainty, it is necessary to consider the power support of various types of power sources to ensure the safe and stable operation of the power system. The general framework of this calculation method includes three steps:

(1) On the basis of combining the load demand of the power system and the installed capacity of different power sources, system load standby, accidental standby and unit overhaul arrangement is carried out.

(2) On the basis of reasonable arrangements for standby and unit maintenance, the working capacity of various types of power sources is determined within a certain time scale by taking into account the system demand and power balance, among which the working capacity of distributed power sources is determined according to a certain guarantee rate.

(3) On the basis of the working capacity of each type of power supply, 8760h of electric power balance calculation is carried out, mainly on the premise of meeting the power balance of each time period, simulating and calculating the complementary relationship between support power sources such as hydroelectricity, thermal power, pumped storage and distributed power sources, the specific idea is to complement each type of support power source within the range of its working capacity and distributed power source, and to give place to the distributed power source when there is distributed power source, without distributed power source. Make way for distributed power supply when there is distributed power supply, and issue power top load when there is no distributed power supply. This power balance calculation method of power support can effectively take into account the characteristics and

uncertainties of various types of power sources, and realize the sustainable utilization and safe and stable operation of distributed power sources. The overall calculation framework is shown in Figure 3.

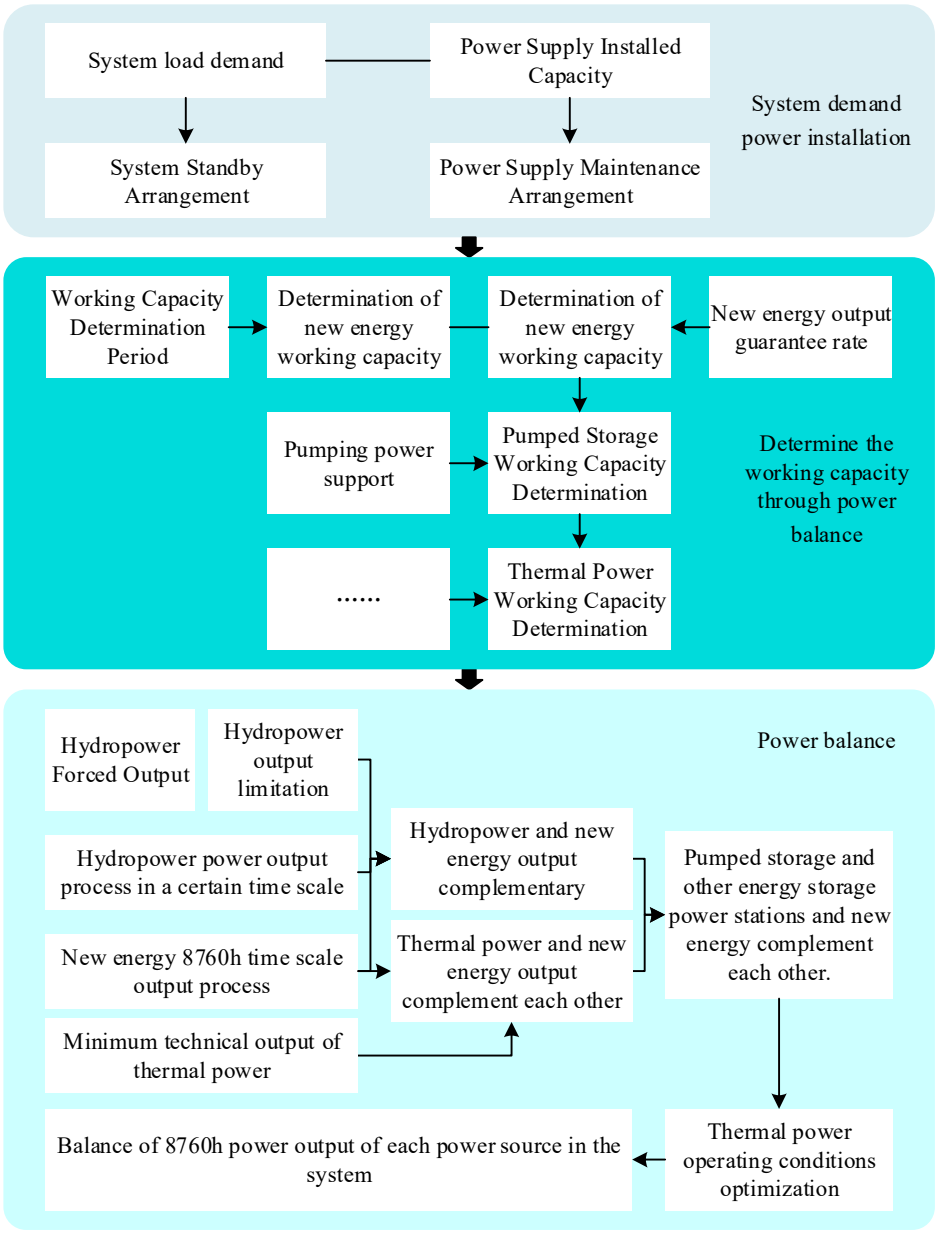

Figure 3: Power balance overall calculation framework

III. A. 2) Electricity power balance calculation model

An electric power balance calculation model is a model used to calculate the balance between supply and demand in an electric power system, and its purpose is to ensure that there is a balance between the amount of power generated in the system and the load demand. The model usually includes the following components:

(1) Generating units: these include various energy generation facilities such as thermal power plants, hydroelectric power plants, and renewable energy facilities such as solar and wind power.

(2) Load: refers to the total demand of all electricity-using devices in the system, including the demand for electricity in various sectors such as industrial, commercial, and residential.

(3) Grid: refers to facilities such as transmission lines and substations that connect generating units and loads.

(4) Energy storage: facilities that include various forms of energy storage, such as batteries, pumped storage, hydrogen storage, etc., in order to provide back-up power in the event of an imbalance between supply and demand. Based on the above components, the electric power balance calculation model can predict the status of supply and

demand balance of the power system in the future period by modeling factors such as output power of generating units, load demand, transmission losses and energy storage, and formulate corresponding scheduling strategies in order to guarantee the stable operation of the power system.

III. B. System electric power balance $N_{\max}$

III. B. 1) Power balance

The basic relational equation for the power balance of a power system at any given moment is:

$$N_{\max} = N_{work} = NH + NT + NE \tag{17}$$

where , N_{work} denote the maximum load and working capacity of the power system, kW, respectively; and NH , NT , and NE denote the working capacity of hydroelectric power plants, thermal power plants, and other power plants, kW, respectively.

III. B. 2) Power balance

The basic relational equation for power system power balance is:

$$E_N = E_W = EH + ET + EE \tag{18}$$

where E_N and E_W denote the amount of electricity needed by the power system and the total generation capacity, $\mathrm{MW \cdot h}$, EH denotes the generation capacity of hydroelectric power plants, $\mathrm{MW \cdot h}$, ET denotes the generation capacity of thermal power plants, $\mathrm{MW \cdot h}$, and EE denotes the electricity generation of other power stations, $\mathrm{MW \cdot h \cdot}$

The distribution of electrical energy among the power stations in the power system is not illustrated by a power balance diagram, so it is also necessary to prepare a power balance diagram. In the power balance, to determine the monthly power station in the annual maximum load map on the working position, which can be analyzed through the monthly typical daily load curve to find the daily power, the power station of the corresponding month of the average daily output that is the daily power divided by 24, multiplied by the monthly adjustment coefficient into the average monthly output, the average monthly output of the power station is plotted in the power system in each month of the annual average load map, that is, the power balance diagram.

Generally take the month as the unit time to carry out the power system power balance, its monthly power generation by the monthly average output. Usually to power power balance diagram to express the results of power power balance, power power balance diagram shows the planning and design of hydropower plants in the power system and the role of the operation of the power system, as well as the degree of utilization of the installed capacity of each station, but also shows the power system throughout the year the power supply situation, and determines the conditions of the unit for the annual overhaul and the degree of guarantee of standby capacity in the system. Finally, the mode of operation is corrected and even the selected installed capacity is adjusted through the preparation of the electricity power balance diagram.

III. B. 3) Principle of calculation of the monthly adjustment factor

The monthly adjustment factor expresses the unevenness of the power station during the month and is expressed as the ratio of the average daily output of the station on a typical day to its average monthly output, viz:

$$k_i = \frac{\overline{P}_i}{\overline{Pm_i}} \tag{19}$$

where k_i denotes the monthly regulation coefficient of power station i ; $\overline{P}_i$ denotes the typical daily average output of power station i , MW; and $\overline{Pm_i}$ denotes the monthly average output of power station i , MW.

The monthly regulation factor of the system is expressed as the ratio of the typical daily average load to the monthly average load of the power system:

$$k = \frac{\overline{N}}{\overline{Nm}} \tag{20}$$

where k and $\overline{N}$ denote the monthly regulation coefficient and typical daily average load of the power system, MW, respectively. $\overline{Nm}$ denotes the monthly average load of the power system, MW.

According to the principle of power and electricity balance of the system, the monthly regulation coefficients and typical daily average outputs of hydroelectric power plants and thermal power plants are described in the power system as follows:

$$k_{H,i} = \frac{\overline{P_{H,i}}}{\overline{Pm_{H,i}}} \tag{21}$$

$$k_{T,j} = \frac{\overline{P_{T,j}}}{\overline{Pm_{T,j}}} \tag{22}$$

$$\overline{P_{H,i}} = f\left(\overline{Nm}, \overline{N}, \overline{Pm_{H,i}}, \overline{Pm_{T,j}}, N_{H,i}^{ava}, N_{T,j}^{ava}, n, m\right) \tag{23}$$

$$\overline{P_{T,j}} = g\left(\overline{Nm}, \overline{N}, \overline{Pm_{H,i}}, \overline{Pm_{T,j}}, N_{H,i}^{ava}, N_{T,j}^{ava}, n, m\right) \tag{24}$$

where $k_{H,i}$, $k_{T,j}$ denote the monthly regulation coefficients of hydropower plant i and thermal power plant j, respectively, and $\overline{P_{H,i}}$, $\overline{P_{T,j}}$ denote the typical daily average outputs of hydropower plant i and thermal power plant j, respectively, in MW. $\overline{Pm_{H,i}}$, $\overline{Pm_{T,j}}$ denote the monthly average output of hydroelectric power plant i and thermal power plant j, respectively, MW. $N_{H,i}^{ava}$, $N_{T,j}^{ava}$ denote the available capacity of hydroelectric power plant i and thermal power plant j, respectively, MW. n denotes the number of hydroelectric power plants, and m the number of thermal power plants.

The formula for calculating the available capacity of hydroelectric power plants and thermal power plants is:

$$N_{H,j}^{ava} = N_{H,j}^{Ins} - R_{H,i} - N_{H,j}^{M} - \overline{Pm_{H,j}} \tag{25}$$

$$N_{T,j}^{ava} = N_{T,j}^{Ins} - R_{T,j} - N_{T,j}^{M} - \overline{Pm_{T,j}} \tag{26}$$

where $N_{H,i}^{Ins}$, $N_{T,j}^{Ins}$ denote the installed capacity of hydropower plant i and thermal power plant j, respectively, in MW. $R_{H,i}$, $R_{T,j}$ denote the standby capacity assumed by hydropower plant i and thermal power plant j, respectively, in MW. $N_{H,j}^{M}$, $N_{T,j}^{M}$ denote the maintenance capacity of hydropower plant i and thermal power plant j respectively, MW.

III. B. 4) Electricity power balance constraints

The monthly power balance expresses the equilibrium relationship between the monthly average output of the power stations in the system and the monthly average load of the system. The power balance for a typical day of the system is represented by the relationship between the typical daily average output of each power station and the typical daily average load of the power system. The monthly power balance and typical day power balance equation constraints are expressed as respectively:

$$\overline{Nm} = \sum_{i=1}^{n} \overline{Pm_{H,i}} + \sum_{j=1}^{n} \overline{Pm_{T,j}} \tag{27}$$

$$\overline{N} = \sum_{i=1}^{n} \overline{P_{H,i}} + \sum_{j=1}^{m} \overline{P_{T,j}} \tag{28}$$

$$\overline{Nm} = \overline{N} / k = \sum_{i=1}^{n} \overline{P_{H,i}} / k_{H,i} + \sum_{j=1}^{m} \overline{P_{T,i}} / k_{T,i} \tag{29}$$

The power balance constraints are divided into two parts, one is the power balance on a typical day, the balance between the maximum load of the power system and the maximum output of each power station on a typical day and the maximum working capacity of the power station. The other part is the balance between the required standby capacity of the power system and the standby capacity assumed by each power station as well as the relationship between the installed capacity, standby capacity, maintenance capacity and working capacity of the power station:

$$N_{\max} = \sum_{i=1}^{n} P_{H,i}^{\max} + \sum_{j=1}^{m} P_{T,j}^{\max} \tag{30}$$

$$R_D = \sum_{i=1}^{n} P_{H,j} + \sum_{j=1}^{m} P_{T,j} \tag{31}$$

$$P_{H,i}^{h} \le N_{H,i}^{\max} \tag{32}$$

$$P_{T,j}^{h} \le N_{T,j}^{\max} \tag{33}$$

$$\overline{Pm_{H,i}} \le \overline{P_{H,i}} \le N_{H,i}^{\max} \tag{34}$$

$$\overline{Pm_{T,j}} \le \overline{P_{T,j}} \le N_{T,j}^{\max} \tag{35}$$

$$N_{H,i}^{\max} = N_{H,i}^{Ins} - R_{H,j} - N_{H,j}^{M} \tag{36}$$

$$N_{T,j}^{\max} = N_{T,j}^{Ins} - R_{T,j} - N_{T,j}^{M} \tag{37}$$

where $N_{\max}$ denotes the maximum load of the power system on a typical day, MW. $P_{H,i}^{h}$, $P_{T,j}^{h}$ denote the output of hydroelectric power plant i and thermal power plant j on a typical day in the h th time period, MW, respectively. h denotes the number of time periods (h takes values from 1-24) and R_D denotes the total standby capacity of the power system, MW. $R_{H,i}$ and $R_{T,j}$ denote the standby capacity of hydroelectric power plant i and thermal power plant j, MW, respectively. $N_{H,i}^{\max}$, $N_{T,j}^{\max}$ denote the maximum working capacity of hydroelectric power plant i and thermal power plant j, MW, respectively.

Monthly adjustment factor constraints:

$$k_{H,i}, k_{T,j} \ge 1 \tag{38}$$

III. C. Novel power system power balance method based on flexible computing

III. C. 1) Modeling of new power systems

This paper takes the new power system as the object, and implements the research on the power system power balance method. At the present stage, the new power system is mainly divided into two key parts: the power unit and the energy storage device, which are also the core components for controlling the power output. In the actual power balance control, the main problem is the instability of the power generation of the new power system. In the limited energy storage space, to ensure that the output power to meet the actual load demand at the same time does not cause ineffective output is the ultimate goal of power system power balance. For this reason, this paper firstly constructs a new type of power system model, denoted as:

$$\begin{aligned} &P_c = C + W \\ &s.t.\ C_{\min} \le C \le C_{\max} \end{aligned} \tag{39}$$

where P_c is the total amount of power generated by the generating units of the new power system, C is the scale of power stored in the energy storage device, W is the scale of power output used to meet the demand of power loads, and $C_{\min}$ and $C_{\max}$ are the lower limit and upper limit of the capacity of the energy storage device, respectively.

Influenced by the renewable energy's own properties in the new power system, P_c is a non-deterministic parameter, so when controlling the power output scale, not only the actual storage state of the energy storage device, but also the actual output of the generating unit should be taken into account. To address this problem, this paper further analyzes the power output of the generator set, and calculates its output state at any moment based on the introduction of the climbing rate, with:

$$P_c(t) = \left(k \sum p\right) \cdot t - \omega_0 \tag{40}$$

where k is the climbing rate of the generating unit, p is the output of a single unit, and ω_0 is the power consumption caused by the operation of the generating unit itself.

Then the new power system model can be expressed as:

$$\begin{aligned} &\left(k\sum p\right)\cdot t-\omega_0=C+W \\ &s.t.\ C_{\min}\le C\le C_{\max} \end{aligned} \tag{41}$$

In this way, the construction of a new type of power system model is accomplished to provide a basis for the subsequent power balance control.

III. C. 2) Balance control of electricity supply and demand based on flexible computing

Using the new power system model constructed above, this paper adopts the flexible calculation to realize the control of the power system power supply and demand balance relationship [27]. It should be noted that, in addition to the dynamic attributes of the generation of generating units, the load demand of the system is also constantly changing according to a certain law. In order to be able to minimize the ineffective power output under the premise of meeting the demand of the power load, this paper takes the load parameters of the power system at any moment as the benchmark, and carries out the flexible complementary calculation of the power output, there:

$$W=f(t) \tag{42}$$

where $f(t)$ is the load parameter at any moment.

Combining the power system model shown in Eq. (41) and substituting Eq. (42) into Eq. (41), it can be obtained:

$$\begin{aligned} &\left(k\sum p\right)\cdot t-\omega_0-C=f(t) \\ &s.t.\ C_{\min}\le C\le C_{\max} \end{aligned} \tag{43}$$

Subject to the limitations of the capacity of the power storage device, the range of values of C is limited, so when $C=C_{\max}$ and the output power of the power system is still greater than the actual load parameters, this paper realizes the regulation and control of the output power by adjusting the climbing rate of the generating unit itself, and the corresponding regulation target can be expressed as follows:

$$k(t)=\frac{f(t)-C_{\max}+\omega_0}{\sum pt} \tag{44}$$

where $k(t)$ is the result of setting the climbing rate of the generating unit when the load parameter of the power system is greater than the current output of the generating unit.

In this way, the power system power is made to realize the balance between supply and demand.

In response to the situation that the total power generation of the generating unit cannot meet the actual power load demand, this paper realizes flexible complementarity by releasing the power in the energy storage device. The specific discharge amount of the energy storage device can be expressed as:

$$\begin{aligned} &C=\left(k\sum p\right)\cdot t-\omega_0-f(t) \\ &s.t.\ C_{\min}\le C\le C_{\max} \end{aligned} \tag{45}$$

When the output of the energy storage device makes its stored power to reach the minimum value, and still can not meet the demand for electricity, the same by adjusting the climbing rate of the generator set itself, to realize the regulation and control of the output power, corresponding to the regulation of the target can be expressed as:

$$k'(t)=\frac{f(t)+C_{\max}+\omega_0}{\sum pt} \tag{46}$$

where $k'(t)$ is the result of setting the climbing rate of the generating unit when the power system load parameter is less than the current generating unit output.

In this way, it is ensured that when the total amount of power generated by the new power system is less than the load demand, the output can also meet the power demand.

According to the above calculation method, combined with the actual operation status of the power system, the adjustment of relevant operation parameters is realized to guarantee the balance of the power system power.

IV. Power balance analysis

IV. A. Flexible balancing calculations

Investigate five typical regions with more obvious characteristics, analyze their power supply situation and load situation by arithmetic example, and the power supply composition of the five regions and their percentage of total power supply are shown in Table 1.

Region A is located in the western region rich in wind and light resources, promoting the construction of new energy sources, the total proportion of wind and light installed capacity is close to thermal power units, and its power supply in addition to meeting the load power supply in the province and the demand for power supply on the Internet, it also bears the burden of inter-provincial and regional power exchange, and needs to bear a certain amount of outgoing power.Region B is located in the more arid northwestern region, and the proportion of small hydropower, biomass power generation and other types of energy is minimal, and the energy composition is dominated by thermal power. Region B is located in the more arid northwestern region, with a very small proportion of other types of energy such as small hydropower and biomass power generation, and the energy composition is dominated by thermal power, and the proportion of new energy is slightly lower than that of region A. Region C is located in the northeastern region, with a very large proportion of traditional thermal power generation, and the total proportion of wind power is close to the proportion of other types of energy, while region D is located in the southern monsoon region, with a large seasonal change of wind power, and the total installed capacity of wind power generation is larger than that of region C. Region E is located in the developed coastal region, and the largest proportion of all energy sources is the offshore wind power, and the power generation capacity of the area is significantly lower than the load, relying on external power deliveries to complete the balance between supply and demand.

Table 1: Composition of power supply in typical areas

Area		Fire power	Wind power	Photovoltaic power	Other
A	Capacity/MW	22446	13026.4	8041.6	8423
	Proportion/%	43.22	25.08	15.48	16.22
B	Capacity/MW	3745	952.4	1024.6	106.5
	Proportion/%	64.25	16.34	17.58	1.83
C	Capacity/MW	32452.4	7023.4	542.8	7546.9
	Proportion/%	68.23	14.76	1.14	15.87
D	Capacity/MW	7642	2030.5	546.2	756
	Proportion/%	69.63	18.50	4.98	6.89
E	Capacity/MW	364.5	416.8	15.3	32
	Proportion/%	43.99	50.30	1.85	3.86

Taking area A as an example, the traditional power balance and the balance calculation of the flexible method are carried out respectively. Firstly, we study the characteristics of wind and light in area A. Collecting and analyzing the historical data of the typical daily power curve in area A, it can be seen that the minimum PV power occurs in the night time, with a value of 0% of the installed capacity, and the maximum power occurs in the summer daytime, with a value of 80% of the installed capacity; the PV power remains higher than the 40% of the installed capacity for nearly two thirds of a day, which can be taken as the flexible lower boundary, flexible upper boundary and flexible center of PV power generation, respectively, in flexible calculations. The lower bound, upper bound and center of flexibility can be taken as the lower bound, upper bound and center of flexibility for PV power generation, respectively.

Similarly, the seasonal variation of wind power output is affected by the climatic conditions of the study area. Area A has a temperate continental climate, and the output reaches the upper limit in spring, which is considered as 60% of the installed capacity, and reaches the lower limit in summer, which is considered as 30% of the installed capacity, and reaches 40% of the installed capacity in autumn and winter, which is taken as the confidence center. Other energy types include biomass power generation, hydropower and nuclear power, etc. Referring to the main grid development planning report of Area A, the minimum output coefficient is taken as 0.4, the maximum output coefficient is taken as 0.8, and the confidence center output coefficient is taken as 0.6. Considering the safety factor when thermal power units are running in summer, the minimum output coefficient is taken as 0.6. The power transmission plan is to transmit 8,000MW of power during the daytime, and one half of the power during the daytime at night. The power is one-half of the daytime power, and the system standby capacity is 2500 MW. Statistics on the operating conditions at different times of the year are made, and then the power surplus level is calculated by subtracting the left side from the right side to obtain the worst case scenario occurring at night in summer, with a power balance of -400 MW, which requires the use of standby capacity. According to the load forecast for this area,

its maximum load on summer nights after 3 years is 24500 MW. To meet the power balance requirement, it can be calculated that at least 4500 MW of new available output is needed.

Then the flexible balance calculation is carried out for the power balance of area A. The results are shown in Table 2. The variation interval of load flexibility parameter is [20350, 25000] MW, and the average value is taken as the flexibility center due to the more uniform load change process.

The left interval of the flexibility inequality is [24524.6, 29684.5] MW, and the right interval is [15023.4, 23875.6] MW, and the minimum value of the left flexibility is larger than the maximum value of the right flexibility, which achieves the condition of flexibility balance. According to the load forecast, the total required load interval after 3 years is [24450, 29200] MW, and the total required power after deducting distributed power generation is [18659.3, 27540.9] MW by the same method, exceeding the minimum value of power-side flexibility by 2896.4 MW, and the newly added available power needs to be greatly reduced compared with the traditional planning method.

Table 2: Calculation of flexible power and energy balance in area A (MW)

Power type	Flexible center	Flexible interval	y-	y+
Fire power	16812	[12574,21050]	4238	4238
Concentrated wind power	2724.3	[1825.6,4375.9]	898.7	1651.6
Distributed wind power	2475.4	[1725.3,3926.7]	750.1	1451.3
Concentrated photovoltaic power	2236.3	[0,4472.6]	2236.3	2236.3
Distributed photovoltaic power	971.4	[0,1942.8]	971.4	971.4
Other	5284.5	[3516,7053]	1768.5	1768.5

Similarly, the power power balance analysis based on flexible arithmetic is performed for the remaining regions. Comparing the excess power on the power supply side obtained by the flexible calculation method with the worst-case excess power on the power supply side of the conventional method in the five regions in the arithmetic example, and calculating the ratio of the difference to the total load in the region, the results are shown in Table 3.

By comparing the results of the flexible balance calculation method with those of the conventional calculation method, it is found that when the total proportion of new energy reaches 40%, the power balance obtained by the flexible planning method is significantly larger than that of the conventional method that generates a deficit. As the proportion of new energy rises, the gap further widens, while the power balance obtained by the conventional method exceeds that of the flexible method when the proportion of new energy decreases due to the decrease in the amount of complementarity of uncertainty intervals. It can be seen that the excess power difference obtained by the two planning methods is positively correlated with the regional new energy share.

Table 3: Results comparison of different power and energy balance methods in five typical areas

Area	Energy range/MW	Power range/MW	Flexible excess power/MW	Traditional excess power/MW	Difference ratio/%
A	[24524.6,29684.5]	[18659.3,27540.9]	1206.4	-400	6.8
B	[3265.2,3987.6]	[2384.4,3045.3]	194.2	334.6	-5.12
C	[24865,38526]	[20648,24386]	552.6	4251.3	-21.68
D	[5984.2,8543.5]	[5012.4,6048.5]	-107.6	-118.5	2.07
E	[425.6,489.7]	[305.4,409.8]	53.7	-12.3	16.24

IV. B. Example studies

IV. B. 1) Overview of examples

In this paper, the power grid of Province Z in Northwest China is selected as a typical power system to analyze the power and electricity balance. According to the relevant plan, in 2030, the power grid of Province Z will have a maximum social load of 70,000 MW, social electricity consumption of 412.5 billion kWh, and the province will gather 8700 MW of grid-to-grid outgoing power and send 53.5 billion kWh of outgoing power.According to the power supply development plan, in 2030, the total installed capacity in Province Z will be 207,300 MW, of which 86,500 MW will be coal-based power (internal grid 58,000MW + 28,500MW of point-to-point grid transmission), accounting for 41.7%. Wind power 40,000MW (39,000MW of provincial transfer + 1,000MW of point-to-grid transmission), accounting for 19.3%. Photovoltaic 68,000MW (62,000MW of provincial regulation + 6,000MW of point-to-grid transmission), accounting for 32.8%. Gas-fired units 3,500MW, accounting for 1.7%. Hydropower 1050MW, accounting for 0.5%. Pumped storage 4000MW, accounting for 1.9%. Biomass power generation 1400MW,

accounting for 0.7%. Other small units 2850MW, accounting for 1.4%. It can be seen that the power grid of Province Z is a power system with a high and new energy share dominated by thermal power.

IV. B. 2) Grid load characteristics and new energy output characteristics

(1) Annual load

According to the relevant power plan of Province Z, the load situation in Province Z in 2030 is shown in Figure 4. The annual load shows a “W” shape, generally characterized by double peaks in summer and winter, and double troughs in spring and autumn, with the two peaks occurring in July and December respectively, and the lowest load in February.

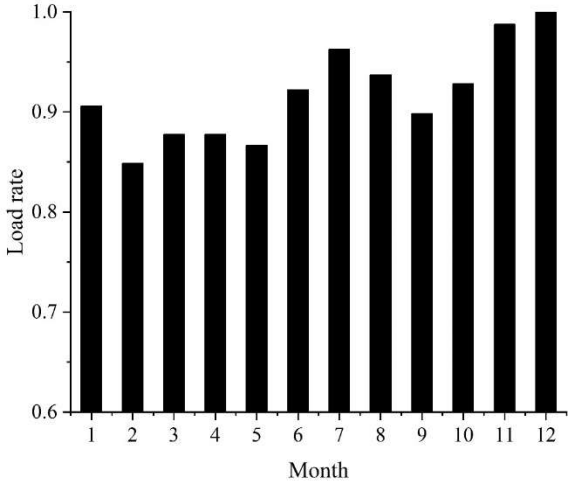

Figure 4: Annual load rate of Z province power grid in 2030

(2) Typical daily load

Typical daily load of power grid in Province Z in 2030 is shown in Figure 5. Basically, it shows the pattern of “double peaks and double valleys”, with the morning peak being more prominent in summer, lasting from 10:00 to 14:00, and the evening peak being more moderate, lasting from 16:00 to 21:00. The evening peak in winter is more prominent than that of the morning peak, with the duration of the morning peak being from 8:00 to 12:00, and the duration of the evening peak being from 17:00 to 21:00. 17:00-21:00.

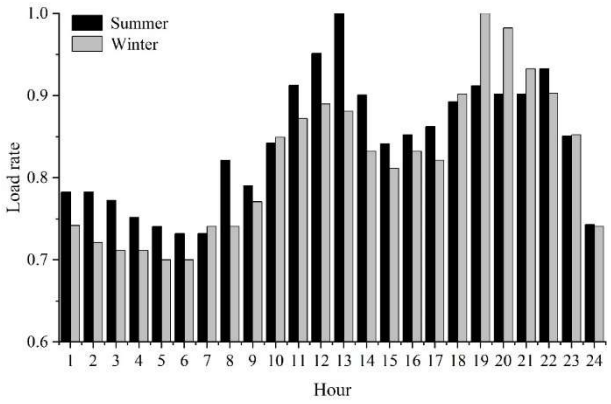

Figure 5: Typical daily load rate of Z province power grid in 2030

(3) Outgoing load

The outgoing curve of Province Z is shown in Fig. 6, which is mainly 6200MW for DC outgoing and 2500MW for EHV AC outgoing.According to the current form of the outgoing curve, the EHV DC channel sends power according to the 100/75 curve, and the power is sent in the four big-load months of January, July, August, and December, and the power is sent in the higher order of the other small-load months according to the capacity of 65%. The UHV AC channel will deliver power according to the 100/70/55 curve throughout the year, but the maximum month of delivery

will be different. 2030, the form of delivery curve will be considered according to the status quo, and only the delivery load will be changed.

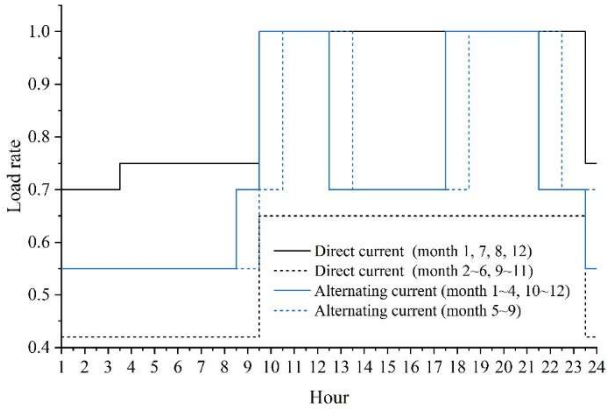

Figure 6: Outbound load curves of Z province power grid in 2030

(4) New energy output characteristics

In 2030, the installed capacity of PV and wind power in Province Z will be 62,000 MW and 39,000 MW respectively, and the curves of annual output characteristics of PV and wind power and the typical daily output characteristics are shown in Fig. 7, of which (a) is the annual output characteristics and (b) is the intra-day output characteristics. From Fig. 7, it can be seen that PV annual spring output is large, winter output is small, and the maximum intraday output is around 13:00. The annual output of wind power is large in winter and small in summer, and the intraday output is large in the evening and small in the daytime.

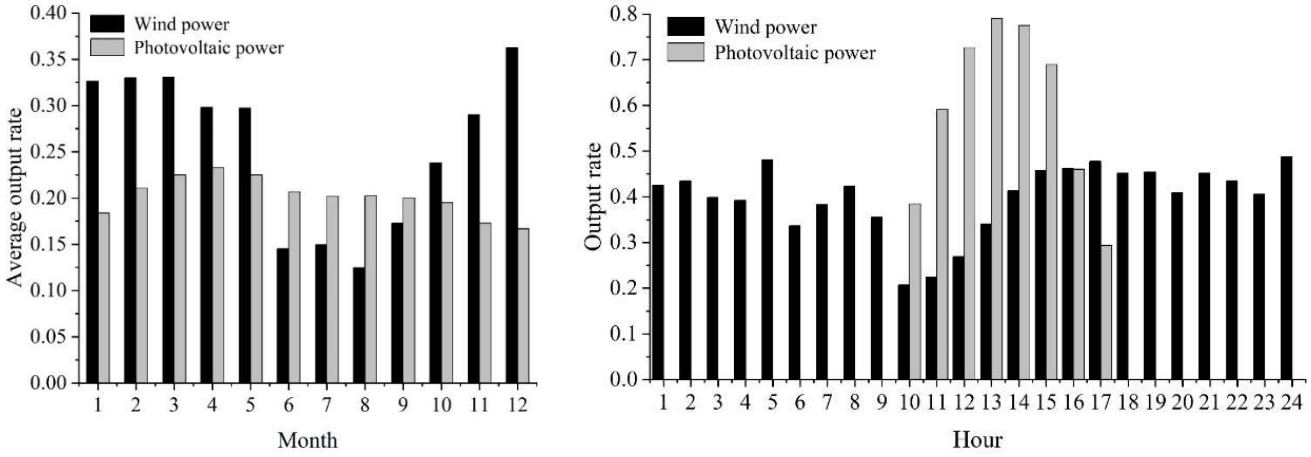

(a) Annual output characteristics

(b) Intra-day output characteristics

Figure 7: Annual and intra-day output characteristics of photovoltaic and wind power

V. Conclusion

In this paper, distributed power supply and electric vehicle charging load are fully considered in the balance calculation of power system, distributed power supply output model and electric vehicle charging load prediction model are constructed, which are embedded in the power system balance calculation model, and the strategy of flexible calculation is adopted to optimize the power system balance calculation method.

(1) The power system balance calculation model constructed in this paper is used to carry out flexible balance calculation for five typical areas, and the variation interval of load flexibility parameters in area A is [20350, 25000] MW, the left interval of flexibility inequality is [24524.6, 29684.5] MW, and the right interval is [15023.4, 23875.6] MW, which realizes the flexible balance After 3 years, the total required load interval is [24450, 29200] MW, and the total required power after subtracting distributed generation is [18659.3, 27540.9] MW, which exceeds the minimum

value of power-side flexibility by 2896.4 MW, and requires at least a significant reduction in the new available power compared to the traditional planning method.

(2) The annual load of the power system in Province Z shows a “W” shape, with double peaks in summer and winter and double valleys in spring and fall. The daily load basically shows the pattern of “double peaks and double valleys”. the UHV DC channel in Province Z delivers power according to the 100/75 curve, and delivers power at full capacity in the four big load months of January, July, August and December, and delivers power at 65% of the capacity in the high order of the other small load months. The UHV AC channel delivers power according to the 100/70/55 curve throughout the year. Photovoltaic annual output is large in spring and small in winter, and the maximum intra-day output is around 13:00. Wind power output during the year is large in winter and small in summer, with large output at night and small output during the day.

Funding

This work was supported by Science and Technology Project of Zhejiang Dayou Group Co., Ltd. (DY2024-11).

References

[1] Zhao, Y., Jian, Z., & Du, Y. (2024). How can China's subsidy promote the transition to electric vehicles?. Renewable and Sustainable Energy Reviews, 189, 114010.
[2] Li, W., Yang, M., & Sandu, S. (2018). Electric vehicles in China: A review of current policies. Energy & Environment, 29(8), 1512-1524.
[3] Wu, Y. A., Ng, A. W., Yu, Z., Huang, J., Meng, K., & Dong, Z. Y. (2021). A review of evolutionary policy incentives for sustainable development of electric vehicles in China: Strategic implications. Energy Policy, 148, 111983.
[4] Islam, A., Ahmed, M. T., Mondal, M. A. H., Awual, M. R., Monir, M. U., & Islam, K. (2021, May). A snapshot of coal‐fired power generation in Bangladesh: a demand–supply outlook. In Natural Resources Forum (Vol. 45, No. 2, pp. 157-182). Oxford, UK: Blackwell Publishing Ltd.
[5] Hemavathi, S., & Shinisha, A. (2022). A study on trends and developments in electric vehicle charging technologies. Journal of energy storage, 52, 105013.
[6] Chen, T., Zhang, X. P., Wang, J., Li, J., Wu, C., Hu, M., & Bian, H. (2020). A review on electric vehicle charging infrastructure development in the UK. Journal of Modern Power Systems and Clean Energy, 8(2), 193-205.
[7] Wolbertus, R., & Van den Hoed, R. (2017). Managing parking pressure concerns related to charging stations for electric vehicles: Data analysis on the case of daytime charging in The Hague. In European Battery, Hybrid & Fuel Cell Electric Vehicle Congress.
[8] Guo, S., Li, P., Ma, K., Yang, B., & Yang, J. (2022). Robust energy management for industrial microgrid considering charging and discharging pressure of electric vehicles. Applied Energy, 325, 119846.
[9] Philipsen, R., Brell, T., Biermann, H., & Ziefle, M. (2019). Under pressure—Users’ perception of range stress in the context of charging and traditional refueling. World Electric Vehicle Journal, 10(3), 50.
[10] Zu, S., & Sun, L. (2022). Research on location planning of urban charging stations and battery-swapping stations for electric vehicles. Energy Reports, 8, 508-522.
[11] Habib, A. A., Hasan, M. K., Mahmud, M., Motakabber, S. M. A., Ibrahimya, M. I., & Islam, S. (2021). A review: Energy storage system and balancing circuits for electric vehicle application. IET Power Electronics, 14(1), 1-13.
[12] Moon, S. K., & Kim, J. O. (2017). Balanced charging strategies for electric vehicles on power systems. Applied Energy, 189, 44-54.
[13] Evzelman, M., Rehman, M. M. U., Hathaway, K., Zane, R., Costinett, D., & Maksimovic, D. (2015). Active balancing system for electric vehicles with incorporated low-voltage bus. IEEE Transactions on Power Electronics, 31(11), 7887-7895.
[14] Habib, A. A., Hasan, M. K., Islam, S., Sharma, R., Hassan, R., Nafi, N., ... & Alotaibi, S. D. (2022). Energy-efficient system and charge balancing topology for electric vehicle application. Sustainable Energy Technologies and Assessments, 53, 102516.
[15] Yang, J. Y., Song, Y. H., & Kook, K. S. (2024). Critical Inertia Calculation Method of Generators Using Energy Balance Condition in Power System. Energies, 17(5), 1097.
[16] Houssein, E. H., Hassan, M. H., Mahdy, M. A., & Kamel, S. (2023). Development and application of equilibrium optimizer for optimal power flow calculation of power system. Applied Intelligence, 53(6), 7232-7253.
[17] Duan, C., Wang, C., Li, Z., Chen, J., Wang, S., Snyder, A., & Jiang, C. (2018). A solar power-assisted battery balancing system for electric vehicles. IEEE transactions on transportation electrification, 4(2), 432-443.
[18] Kahlen, M. T., Ketter, W., & van Dalen, J. (2018). Electric vehicle virtual power plant dilemma: Grid balancing versus customer mobility. Production and Operations Management, 27(11), 2054-2070.
[19] Duraisamy, T., & Kaliyaperumal, D. (2021). Machine learning-based optimal cell balancing mechanism for electric vehicle battery management system. IEEE Access, 9, 132846-132861.
[20] Hoque, M. M., Hannan, M. A., Mohamed, A., & Ayob, A. (2017). Battery charge equalization controller in electric vehicle applications: A review. Renewable and Sustainable Energy Reviews, 75, 1363-1385.
[21] Rivera, S., & Wu, B. (2016). Electric vehicle charging station with an energy storage stage for split-DC bus voltage balancing. IEEE Transactions on Power Electronics, 32(3), 2376-2386.
[22] Huang, Y., Masrur, H., Lipu, M. S. H., Howlader, H. O. R., Gamil, M. M., Nakadomari, A., ... & Senjyu, T. (2023). Multi-objective optimization of campus microgrid system considering electric vehicle charging load integrated to power grid. Sustainable Cities and Society, 98, 104778.
[23] Zhang, Z., Shi, H., Zhu, R., Zhao, H., & Zhu, Y. (2021). Research on electric vehicle charging load prediction and charging mode optimization. Archives of Electrical Engineering, 399-414.
[24] Teyang Zhao,Hui Liu,Jinshuo Su,Ni Wang & Zhiqiang Luo. (2025). Coordinated control for distributed energy resources in Islanded microgrids with improved frequency regulation capability. Renewable Energy,244,122690-122690.
[25] Tianci Lu,Hao Wu,Shuiming Yin & Xiaoli Xu. (2024). Study of Rock Damage Constitutive Model Considering Temperature Effect Based on Weibull Distribution. Applied Sciences,14(9).

[26] Weixiu Lin,Feng Li,Junjie Gong,Lingwei Yu,Jun Lu,Bin Zhang... & Lei Ni. (2024). Optimization and improvement method for complementary power generation capacity of wind solar storage in distributed photovoltaic power stations. Journal of Physics: Conference Series,2814(1),012011-012011.

[27] Bo Liang,Lei Xie,Hanqi Li,Xiaohui Liu,Zixu Wang & Jiaqi Zhang. (2024). Optimization Method of Electricity Package Settlement for Complex Users Based on Flexible Computing Algorithm. Journal of Physics: Conference Series,2774(1).